Observation of a Laser-Induced Resonance in the Photoionization Spectrum of Sodium

S. Cavalieri[a] and F. S. Pavone
European Laboratory for Non-linear Spectroscopy (LENS), Largo E. Fermi 2, I-50125 Firenze, Italy

M. Matera
Istituto di Elettronica Quantistica, Consiglio Nazionale delle Ricerche, Via Panciatichi 56/30, I-50127 Firenze, Italy
(Received 4 September 1991)

We report the observation of a structure in the ionization spectrum of sodium, induced by a strong radiation field embedding the $5s\ ^2S_{1/2}$ state into the continuum. The structure, probed by single-photon ionization, shows a marked asymmetry, typical of a laser-induced continuum structure.

PACS numbers: 32.80.Rm, 32.80.Wr

Since the theoretical treatment of autoionization proposed by Fano in 1961 [1], the coherent interaction of atoms with a radiation field, coupling low-lying bound states to the ionization continuum, has attracted the interest of scientists. In fact, the asymmetric line shape of a Fano resonance is a manifestation of quantum-mechanical interference between two transition pathways leading to the same continuum state: direct photoionization, on one side, and transition to the continuum via the (discrete) autoionizing state, on the other side. The coherent population trapping occurring in transitions involving autoionizing states appears of great interest today for the study of atomic systems which may provide lasing in the absence of population inversion [2].

Heller and Popov in 1976 [3] showed that a featureless ionization continuum can be structured by a strong laser field embedding a low-lying bound state in the continuum. The dressing of continuum states by the radiative coupling to the bound state gives rise to an "autoionizing-like" resonance, which can be probed by a weak radiation field [Fig. 1(a)]. The peculiar property of this structure, which is termed laser-induced continuum structure (LICS), is that its position can be varied by simply tuning the frequency of the dressing laser. Expected applications of LICS are the control of photoionization rates, the enhancement of nonlinear frequency mixing, and the production of spin-polarized electrons by multiphoton ionization [4].

In contrast to the extensive theoretical work devoted to the subject [5,6], only few experiments have been reported in the literature, showing results that are sometimes not consistent with each other nor with theoretical predictions.

The first evidence of LICS was the observation of optical-polarization rotation in the neighborhood of a resonance induced by σ-polarized radiation in cesium [7]. The technique, well known in polarization spectroscopy, is highly sensitive because the extinction ratio of commercial polarizers, which is better than 10^{-5}, allows a true zero measurement. Recent experimental results [8], confirming the observation of the effect, have shown that a deeper study is needed to relate the observed line shape to the atomic parameters and to the interaction dynamics. LICS has also been used to enhance third-harmonic generation in sodium vapor [9]. However, no structure has been observed in subsequent experiments, carried out in different laboratories [10,11]. Zhang and Lambropoulos [12] have performed a theoretical study of the problem, showing how the temporal evolution and the relative spatial intensity distribution of the laser fields, which are difficult to control in the case of multimode lasers, play a crucial role in making the LICS observable, above the statistical fluctuation of the third-harmonic signal. A systematic ionization study of laser-induced resonances in the multiphoton ionization spectrum of sodium has been made by Feldmann *et al.* [13]. Although reporting the observation of five-photon resonances, due to Raman-type processes involving near-resonant bound states, they found no conclusive evidence for asymmetric resonances. Not even the resonance studied in the third-harmonic experiment mentioned above was observed.

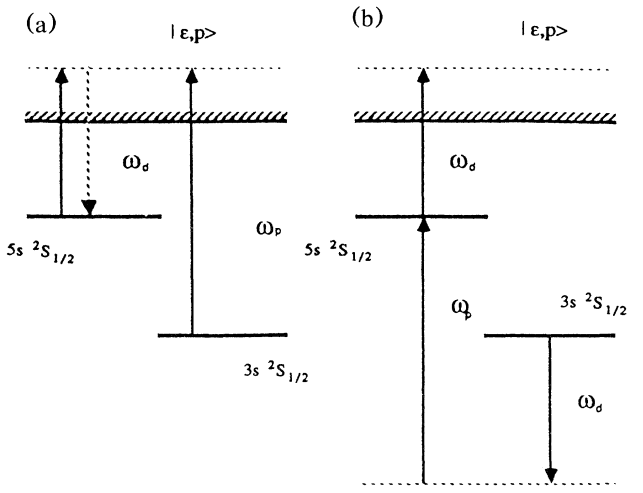

FIG. 1. Schemes of the lowest-order transition pathways coupling the $3s$ and the $5s$ states of sodium to the ionization continuum $|\varepsilon,p\rangle$ in the presence of a strong dressing laser and a weak probe laser with frequencies ω_d and ω_p, respectively. The bound states can be coupled to each other (a) through the continuum or (b) by a Raman process, through a nonresonant virtual state.

To our knowledge, the only direct observation of LICS in the ionization spectrum has been reported by Hutchinson and Ness for xenon [14]. The laser-induced structure, probed by two-photon-resonant, three-photon ionization, was found over a pronounced background, due to ionization of the two-photon resonant level by the dressing laser. Since the experiment was performed under conditions of strong fields and high xenon density with significant collisional and collective effects, the measured line shape did not allow the quantitative comparison with theory needed for a better understanding of LICS [15].

In this paper we report the observation of a laser-induced resonance in the single-photon ionization spectrum of sodium, as shown in Fig. 1(a), where ω_d is the frequency of the dressing laser, embedding the $5s\ ^2S_{1/2}$ state in the $|\varepsilon,p\rangle$ continuum, and ω_p is the frequency of a weak laser, probing the structure by photoionization of the ground $3s\ ^2S_{1/2}$ state. The states $3s$ and $5s$ can also be coupled to each other through the nonresonant Raman process of Fig. 1(b). Both transition pathways can affect the ionization, subject to the resonance condition

$$\omega_p - \omega_d = [E(5s) - E(3s)]/\hbar\ . \qquad (1)$$

The Raman coupling, even away from resonance, can be as important as the coupling through the continuum [16]. Since the relative contribution of the Raman and LICS processes depends only on the properties of the specific system, predictions not derived from atomic calculations can be misleading, as stressed in Ref. [16].

The advantage of single-photon probing is evident in the fact that only one Raman process, through a virtual state detuned by ω_d from the ground state, can be involved.

The experimental arrangement is schematically shown in Fig. 2. The laser beams are generated by a commercial dye laser pumped by the second harmonic of a Q-switched pulsed Nd:YAlG laser (YAlG denotes yttrium aluminum garnet). The pump laser (Quantel model YG-581-C), consisting of an injection seeded Gaussian oscillator, followed by a 9-mm-diam amplifier, provides

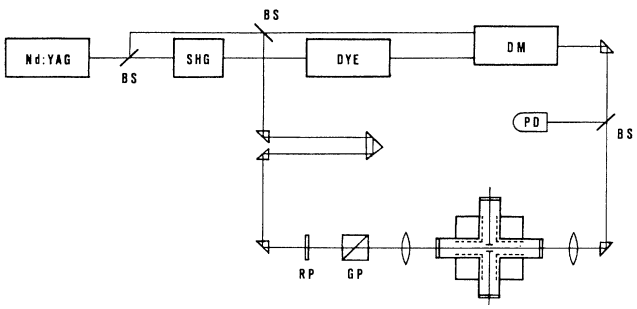

FIG. 2. Schematic diagram of the experimental apparatus: SHG, second-harmonic generator; DM, optical doubling-mixing system; PD, monitor photodiode; BS, beam splitter; RP, $\lambda/2$ retarding plate; GP, Glan polarizer.

single-mode smooth pulses at $\lambda = 1064$ nm with 1 J energy, 6 nsec duration (FWHM), and 0.003 cm^{-1} bandwidth. Efficient second-harmonic generation in a temperature stabilized potassium dihydrogen phosphate (KDP) crystal provides pulses at $\lambda = 532$ nm suitable for dye pumping. The dye laser (Quantel model TDL-50) consists of a multimode oscillator, equipped with a four-prism beam expander, followed by two amplification stages. Operated with a mixture of rhodamine 640 and 610, it provides 50-mJ pulses of linearly polarized radiation tunable around $\lambda = 602.3$ nm (two-photon resonance with the $5s$ state). As a result of mode beating in the oscillator cavity, the temporal profile of the dye output is not smooth, presenting a modulation, with period of ≈ 2 nsec and depth $\approx 30\%$ of the average amplitude, fluctuating from pulse to pulse. Finally, as a result of sum mixing between the Nd:YAlG emission and the second harmonic of the dye emission, we get pulses of tunable radiation at $\omega_p = \omega_{ir} + 2\omega_{dye}$ ($\lambda \approx 234.7$ nm), with maximum energy ≈ 1 mJ, bandwidth ≈ 0.2 cm^{-1}, and temporal duration ≈ 4 nsec (FWHM). The laser fields at different frequencies are separated by a Pellin-Broca prism. The resolution and resettability of the frequency scanning system are better than the emission bandwidth. The doubling-mixing facility is equipped with a tracking system, providing a continuous adjustment of the KDP crystal orientations during frequency scans.

A fraction of the Nd:YAlG output, reflected by a beam splitter, is used as the dressing laser. The probe and the dressing beams, focused by 20- and 30-cm focal length lenses, respectively, overlap in the center of the heat pipe, in a counterpropagating geometry. Optimum timing is provided by an optical delay line on the dressing beam, whose polarization is rotated in order to be parallel to that of the probe beam. The beam waists have been measured to both be ≈ 50 μm. Sodium is evaporated in a stainless-steel cross heat pipe: Argon buffer gas provides vapor confinement, preventing deposition on the water-cooled fused silica windows. Two round electrodes of 7 mm diameter are inserted in the heat pipe by the side arms with a separation of 3 mm in order to measure with maximum efficiency the ionization produced by the probe beam in the waist region of the dressing beam. The probe laser is properly attenuated to avoid ionization saturation, space-charge effects, and other spurious effects described below. The charge signal, with a repetition rate of 10 pulses/sec, detected by a fast transimpedance amplifier is measured by using an SRS synchronous integrator (model SR 250) with a 1-μsec gate width, interfaced to an IBM XT-286 PC for data acquisition and processing. The signal from a monitor photodiode on the UV laser beam is used to perform a pulse-by-pulse normalization of the charge signal.

Figure 3 shows the ionization spectra obtained by varying the probe-laser frequency ω_p, and probe- and dressing-laser energies. In the figure we have plotted the ion-

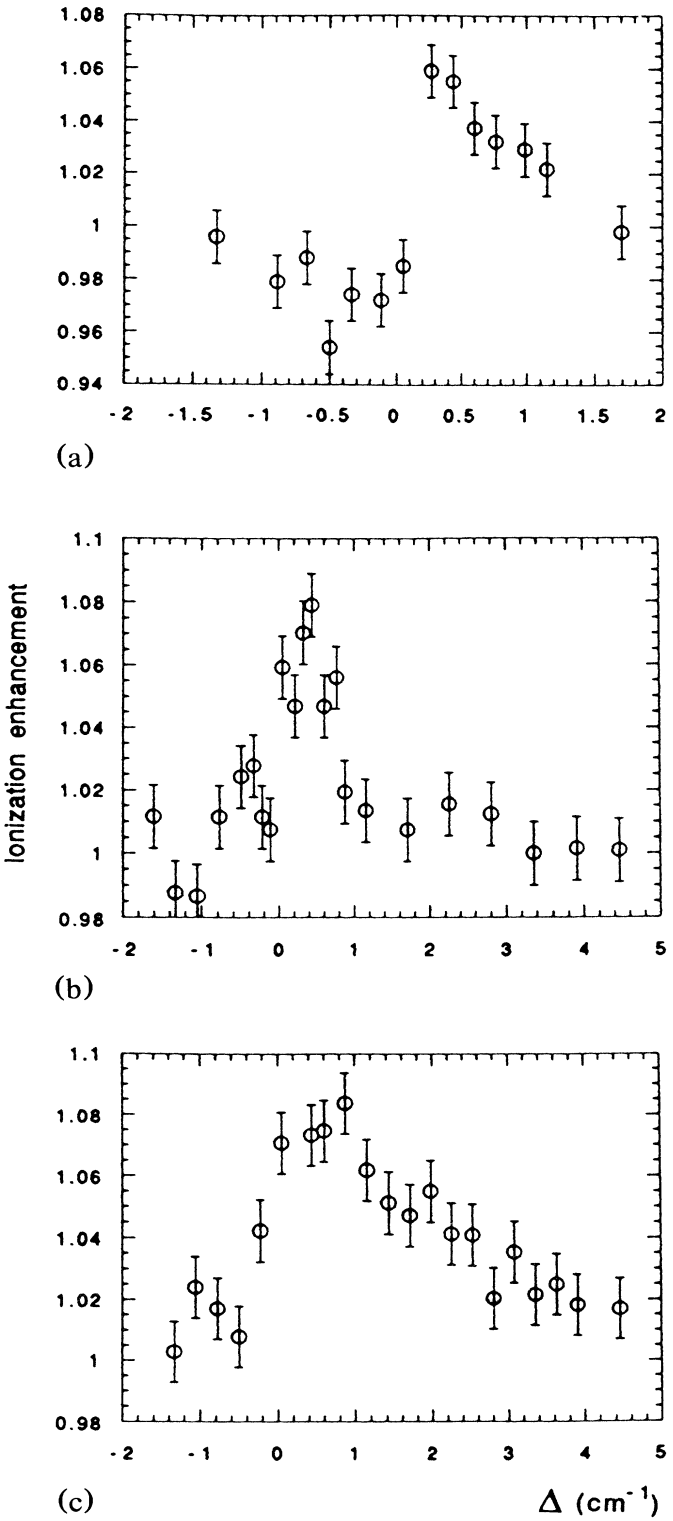

FIG. 3. Plot of the ionization enhancement vs the laser detuning Δ for different probe- and dressing-field energies: (a) $E_p \approx 5$ μJ ($I_p \approx 64$ MW/cm^2), $E_d \approx 1.5$ mJ ($I_d \approx 13$ GW/cm^2); (b) $E_p \approx 50$ μJ, $E_d \approx 1.5$ mJ; (c) $E_p \approx 50$ μJ, $E_d \approx 5$ mJ.

ization enhancement defined as ratio of the ionization signal measured in the presence of dressing laser to that measured in the absence of dressing laser, versus the laser detuning from the Raman resonance:

$$\Delta = (\omega_p - \omega_d) - [E(5s) - E(3s)]/\hbar . \quad (2)$$

At resonance ($\Delta = 0$) the emission of the dye laser is two-photon resonant with the $3s$-$5s$ transition. The measurement of the profile of this two-photon resonance, observed in the three-photon ionization spectrum, has provided an absolute calibration of the detuning scale. The ionization signal, normalized to the probe-laser energy E_p, is averaged over 200 laser pulses. The heat pipe was operated at a temperature of 300 °C, with about 30 mbar of buffer gas, providing a sodium density $\approx 2 \times 10^{14}$ atoms/cm^3 in a region of about 10 cm length.

A sensitivity of about 10^{-2} in the measurement of the ionization enhancement was made possible by a careful optimization of the experimental conditions, performed with the purpose of minimizing the background. For a reduction of the ionization produced by the dressing laser alone, due to multiphoton ionization of atoms and clusters, the choice of the physical system, sodium dressed by the fundamental emission of the Nd:YAlG laser (instead of its second harmonic), was crucial. The geometrical configuration of the electrodes was then very effective in making negligible ($< 10^{-3}$ times the ionization induced by the probe laser) the residual background, mainly due to ionization of clusters in the cold parts of the cell, where vapor condensation takes place. However, in conditions of high laser intensities and/or high sodium density, the dressing laser gives rise to a nonresonant enhancement of the ionization produced by the probe laser, greatly reducing the sensitivity of the measurement. An analysis of the effect suggested, as a possible cause, an avalanche multiplication of the original photoelectrons accelerated in the oscillating field of the dressing laser. This interpretation was confirmed by the observation, in particular conditions, of spikes in the ionization signal, occurring only when both lasers were present and overlapped in the interaction region, revealing a laser-induced breakdown of the photoionized gaseous medium. In our spectra this effect was carefully avoided, as shown by the fact that, out of resonance, the ionization enhancement approaches 1.

For low probe-field intensity [Fig. 3(a)] the line shape is markedly asymmetric, with an ionization suppression on the negative detuning side, indicating that, in spite of the spatial and temporal field distribution, some coherent population trapping takes place. At increased probe intensity [Fig. 3(b)] the ionization window is less evident above the statistical fluctuation, making the line shape more symmetric. An explanation of this effect might be found in ionization pathways different from those shown in Fig. 1(a), as the ionization of the $5s$ state due to the probe laser [6]. At higher dressing-field intensity [Fig.

3(c)] the resonance is found wider and significantly asymmetric, with an enhanced tail on the positive detuning side.

Following theoretical models of LICS, an estimation of the resonance width is given by

$$\Gamma = \gamma_{lp} + \gamma_{ld} + \sum \gamma_{\mathrm{ph}} , \quad (3)$$

where γ_{ph} are the photoionization rates of the ground and $5s$ states in the presence of the probe and dressing lasers, and γ_{lp} and γ_{ld} are the contributions from the bandwidths of the probe and dressing lasers. Radiative damping of state $5s$ is neglected since the natural lifetime (78 nsec) is much larger than the laser pulse duration (4 nsec).

In our conditions (weak probe field and negligible multiphoton ionization of the ground state from the dressing laser) the main γ_{ph} is the photoionization rate of the $5s$ state due to the dressing laser:

$$\gamma_{\mathrm{ph}} = (\sigma_{5s,\varepsilon}/ch\omega_d) I_d = 0.043 I_d \ \mathrm{cm}^{-1} , \quad (4)$$

where $\sigma_{5s,\varepsilon}$ is the cross section of photoionization of the state $5s$ for the radiation at $\lambda = 1064$ nm and I_d is given in GW/cm^2. The value of $\sigma_{5s,\varepsilon}$, equal to 1.49 ± 0.13 Mb, is an experimental datum from Ref. [17]. Considering that $\gamma_{lp} + \gamma_{ld} \approx 0.2$ cm^{-1}, we get the values $\Gamma \approx 0.76$ cm^{-1} for $E_d = 1.5$ mJ and $\Gamma \approx 2.05$ cm^{-1} for $E_d = 5$ mJ, which are consistent with the line shapes of the measured spectra. The comparison of the peak value of the ionization enhancement, which is about 8×10^{-2}, with theoretical predictions should be done considering that in the experiment the beam waists of the probe and dressing lasers were comparable, so that the photoionization induced by the probe laser was presumably not affected by the dressing laser in the overall interaction region. A quantitative interpretation of the experimental results, based on numerical calculations, taking into account the actual interaction conditions, is in progress.

In conclusion, we have reported the first observation of a laser-induced resonance in the single-photon ionization spectrum of sodium. The accuracy of the measurement has provided clear evidence for an asymmetric line shape typical of the laser-induced continuum structure. When the work was completed we were informed that evidence for a laser-induced structure in the single-photon ionization spectrum of sodium has been obtained in an atomic beam experiment [18]. The study of laser-induced resonances in single-photon ionization experiments, performed either in a heat pipe or in atomic beams, can provide quantitative tests for theoretical models of LICS.

The research has been carried out at the European Laboratory for Non-linear Spectroscopy (LENS). It is a pleasure to acknowledge many helpful discussions with Professor P. Lambropoulos. We also thank Dr. R. Buffa for stimulating our interest in LICS. The valuable technical assistance of R. Ballerini and M. Giuntini is greatly appreciated.

[a] Also at Dipartimento di Fisica, Università di Firenze, Largo E. Fermi 2, I-50125 Firenze, Italy.

[1] U. Fano, Phys. Rev. **124**, 1866 (1961).
[2] S. E. Harris, Phys. Rev. Lett. **62**, 1033 (1989); V. G. Arkhipkin and Yu. I. Heller, Phys. Lett. **98A**, 12 (1983).
[3] Yu. I. Heller and A. K. Popov. Opt. Commun. **18**, 449 (1976).
[4] G. Alber and P. Zoller, Phys. Rev. A **27**, 1713 (1983).
[5] Yu. I. Heller and A. K. Popov, J. Sov. Laser Res. **6** (1985).
[6] P. L. Knight, M. A. Lauder, and B. J. Dalton, Phys. Rep. **190**, 1 (1990), and references therein.
[7] Yu. I. Heller, V. F. Lukinykh, A. K. Popov, and V. V. Slabko, Phys. Lett. **82A**, 4 (1981).
[8] S. Cavalieri, M. Matera, and F. S. Pavone (to be published).
[9] L. I. Pavlov, S. S. Dimov, D. I. Metchkov, G. M. Mileva, K. V. Stamenov, and G. B. Altshuller, Phys. Lett. **89A**, 441 (1982).
[10] P. B. Chapple, Ph.D. thesis, Australian National University, 1988 (unpublished).
[11] S. Cavalieri, M. Matera, and F. S. Pavone (unpublished).
[12] J. Zhang and P. Lambropoulos (to be published).
[13] D. Feldmann, G. Otto, D. Petring, and K. H. Welge, J. Phys. B **19**, 269 (1986).
[14] M. H. R. Hutchinson and K. M. M. Ness, Phys. Rev. Lett. **60**, 105 (1988).
[15] X. Tang, A. L'Huillier, and P. Lambropoulos, Phys. Rev. Lett. **62**, 111 (1989); M. H. R. Hutchinson and K. M. M. Ness, Phys. Rev. Lett. **62**, 112 (1989).
[16] Bo-nian Dai and P. Lambropoulos, Phys. Rev. A **36**, 5205 (1987).
[17] A. V. Smith, J. E. M. Goldsmith, D. E. Nitz, and S. J. Smith, Phys. Rev. A **22**, 577 (1980).
[18] Y. L. Shao, D. Charalambidis, C. Fotakis, Jian Zhang, and P. Lambropoulos, preceding Letter, Phys. Rev. Lett. **67**, 3669 (1991).